

Tsallis Entropy In Bi-level And Multi-level Image Thresholding

*Original*

Tsallis Entropy In Bi-level And Multi-level Image Thresholding / Sparavigna, Amelia Carolina. - In: INTERNATIONAL JOURNAL OF SCIENCES. - ISSN 2305-3925. - STAMPA. - 4:1(2015), pp. 40-49.

*Availability:*

This version is available at: 11583/2590164 since:

*Publisher:*

England: Alkhaer Publications

*Published*

DOI:

*Terms of use:*

This article is made available under terms and conditions as specified in the corresponding bibliographic description in the repository

*Publisher copyright*

default\_article\_editorial [DA NON USARE]

-

(Article begins on next page)

## Tsallis Entropy in Bi-level and Multi-level Image Thresholding

Amelia Carolina Sparavigna<sup>1</sup>

<sup>1</sup>Department of Applied Science and Technology, Politecnico di Torino, Italy

**Abstract:** The maximum entropy principle has a relevant role in image processing, in particular for thresholding and image segmentation. Different entropic formulations are available to this purpose; one of them is based on the Tsallis non-extensive entropy. Here, we propose a discussion of its use for bi- and multi-level thresholding.

**Keywords:** Image Processing, Tsallis Entropy, Thresholding

### 1. Introduction

In 1988, Constantino Tsallis proposed, in a paper entitled "Possible generalization of Boltzmann–Gibbs statistics" [1], a new concept of entropy, which is known today as "Tsallis entropy". This entropy was embedded in a generalization of the classical statistics, formulated for a non-extensive thermodynamics. For systems with long-range interactions or long time memory, Tsallis used an approach which was inspired by some multifractals concepts. As the scaling functions of the universal multifractals are depending on a multifractality index, the Tsallis entropy depends on a dimensionless parameter; when this parameter has the limit value of 1, the entropy is recovering the expression of Boltzmann–Gibbs entropy.

Today, we can see that a strongly increasingly number of natural and artificial systems is studied by means of Tsallis entropy [2]: of all the researches referring to it, a large part, at least more than a thousand, are on its application in image processing. The Tsallis entropy enters the image processing through the problem of image segmentation. This is a processing task which aims separating the image pixels in some manner, for instance, in pixels pertaining to objects or to the background. This very important process is the first step to understand the components of the image and for a recognition and extraction of their features [3].

The segmentation can be made by image thresholding, usually classified as bi-level and multi-level thresholding. Bi-level thresholding separates the pixels into two classes, one containing pixels with gray-levels below the threshold, the other with gray-levels above it. Multi-level thresholding generalizes this to several classes [3]. Here, we will discuss the use of Tsallis entropy in bi- and multi-level image thresholding.

### 2. Tsallis entropy and non-additivity

Let us have a discrete set of probabilities  $\{p_i\}$ , where  $i$  is a discrete random variable. Condition on probabilities is:  $\sum_i p_i = 1$ . For any real parameter  $q$ ,

Tsallis entropy is defined as:

$$S_q(p_i) = \frac{k}{q-1} \left( 1 - \sum_i p_i^q \right) \quad (1)$$

Sometimes, parameter  $q$  appearing in (1) is named the "entropic index".  $k$  is a constant.

In the limit  $q \rightarrow 1$ , the usual Boltzmann–Gibbs entropy is recovered, namely:

$$S_{BG} = S_1 = -k \sum_i p_i \log p_i \quad (2)$$

In the case this entropy is used in information theory, it assumes the form of the Shannon entropy ( $k = 1$ ):

$$S_S = - \sum_i p_i \log p_i \quad (3)$$

The Tsallis Entropy has been used along with the principle of maximum entropy to derive Tsallis distributions. For instance, the  $q$ -Gaussians are the distributions maximizing the entropy, having the same role of Gaussians in the Boltzmann–Gibbs theory.

The Boltzmann–Gibbs and Shannon (BGS) statistics is naturally applied to systems having short-range microscopic interactions and microscopic memory. Systems obeying BGS statistics are called extensive systems. Let us consider a physical system decomposed into two independent systems A and B,



having joint probability:  
 $p(A, B) = p(A)p(B)$ , BGS entropy is additive:

$$S_{BGS}(A, B) = S_{BGS}(A) + S_{BGS}(B) \quad (4)$$

In the case Tsallis entropy is evaluated, we have:

$$S_q(A, B) = S_q(A) + S_q(B) + (1-q)S_q(A)S_q(B) \quad (5)$$

The Tsallis entropy possesses the remarkable property of being non-additive. It means that the concerned systems are non-extensive. Modulus  $|1-q|$  is measuring the departure from additivity. In the limit when  $q \rightarrow 1$ , we have the expected additivity of entropy. Note that parameter  $q$  can be lesser or greater than 1. In the case  $q < 1$ , the entropy is subextensive:  $S_q(A, B) < S_q(A) + S_q(B)$ . When  $q = 1$ , it is extensive and when  $q > 1$ , it becomes superextensive:  $S_q(A, B) > S_q(A) + S_q(B)$ .

In fact, Costantino Tsallis and Alfred Renyi both proposed entropies that, for  $q = 1$ , reduce to the Shannon entropy. The Renyi entropy is defined as [4]:

$$\bar{S}_q(p_i) = \frac{1}{1-q} \ln \left( \sum_i p_i^q \right) \quad (6)$$

This entropy is additive and the parameter  $q$  is used to have it more or less sensitive to the shape of probability [5]. The link between Tsallis and Renyi entropy is given in [1]:

$$\bar{S}_q \equiv \frac{1}{1-q} \ln [1 + (1-q)S_q] \quad (7)$$

Let us assume two independent systems A and B again. Since the Renyi entropy is additive:

$$\bar{S}_q(A, B) = \bar{S}_q(A) + \bar{S}_q(B) \quad (8)$$

Using (7) in (8), we have Eq.5.

Let us remember also that in 1967, Havrda and Charvát defined an entropy [6]:

$$S_q^{HC} = \frac{1}{1-2^{1-q}} \left( 1 - \sum_i p_i^q \right) \quad (9)$$

This entropy differs from that proposed independently by Tsallis for the normalization factor. The Havrda and Charvát entropy is normalized to 1, whereas the Tsallis entropy is not normalized. As told in [7], for the use made in the reference, both entropies yield the same result and for this reason the entropy is also named Tsallis–Havrda–Charvát entropy.

### 3. Entropy, information and images

Before Tsallis had proposed his entropy, the use of maximum entropy principle was already considered a powerful method for image processing and reconstruction. As explained in [8], the method had the privileged position of being the only consistent method for combining different data into a single image. In fact, the maximum entropy method allows incorporating extra knowledge about the object which is represented in the image.

In 2000, Takuya Yamano generalized the Shannon's information theory in a non-additive way, and proposed this generalization in a work [9] where he explored the consequences of adopting a non-additive information content and a non-additive entropy. In 2003, this generalization was extended to image processing areas, specifically to image segmentation [10].

One of the simplest methods used for segmentation is the thresholding. In [11], a survey of thresholding is given, which is categorizing the methods into some groups based on the information the algorithms are manipulating. Among them, we find methods based on histograms of the gray-level sample or methods based on clustering, where the gray-level samples are clustered in two parts as background and objects. We have also the entropy-based methods: as told in [10], Kapur et al. [12] assumed two probability distributions, one for the object and the other for the background and maximized the total entropy of the partitioned image in order to obtain the threshold level. In [10], the authors used a method similar to the maximum entropy sum method of Kapur et al., however, using the Tsallis entropy.

### 4. Entropy of an image

Let us consider an image having  $k$  gray levels. Let  $f(x, y)$  be the gray value of the pixel located at the point  $(x, y)$ . In fact, a digital image of size  $X \times Y$  is a matrix of the form  $[f(x, y) | x = 1, 2, \dots, X; y = 1, 2, \dots, Y]$ . Let the set of all gray values  $\{0, 1, 2, \dots, k\}$ . Usually,  $k = 255$ .

We need a distribution of probabilities,  $p_1, p_2, \dots, p_k$ . To have it we use the histogram of the gray values. The normalized histogram is:

$$h(i) = \frac{N_i}{N_{tot}} \quad (10)$$

$N_i$  is the number of pixels with gray value  $i$  and  $N_{tot}$  is the number of all pixels in the image. The probability distribution is:

$$I: \frac{p_1}{p_o}, \frac{p_2}{p_o}, \dots, \frac{p_k}{p_o} \quad (11)$$

$$p_o = \sum_{i=1}^k p_i = 1 \quad (12)$$

Note that (11) is estimated by:

$$I: h(1), h(2), \dots, h(k) \quad (13)$$

The Tsallis entropy is:

$$S_q^I = \frac{1}{q-1} \left\{ 1 - \sum_{i=1}^k h(i)^q \right\} \quad (14)$$

Let us stress again that Tsallis entropy is a function of parameter  $q$ .

### 5. Entropic segmentation via thresholding

Let us consider again an image having  $k$  gray levels, with a distribution of probabilities,  $p_1, p_2, \dots, p_k$ .

Let us assume a bi-level threshold  $t$  for the gray levels. In [10], two classes had been introduced, A and B, and their probability distributions:

$$A: \frac{p_1}{p_A}, \frac{p_2}{p_A}, \dots, \frac{p_t}{p_A} \quad (15)$$

$$B: \frac{p_{t+1}}{p_B}, \frac{p_{t+2}}{p_B}, \dots, \frac{p_k}{p_B} \quad (16)$$

In (15) and (16), we have:

$$p_A = \sum_{i=1}^t p_i; p_B = \sum_{i=t+1}^k p_i \quad (17)$$

The Tsallis entropy for each distribution is:

$$S_q^A(t) = \frac{1}{q-1} \left\{ 1 - \sum_{i=1}^t \left( \frac{p_i}{p_A} \right)^q \right\} \quad (18)$$

$$S_q^B(t) = \frac{1}{q-1} \left\{ 1 - \sum_{i=t+1}^k \left( \frac{p_i}{p_B} \right)^q \right\} \quad (19)$$

The entropy is:

$$S_q(t) = S_q^A(t) + S_q^B(t) + (1-q) S_q^A(t) S_q^B(t) \quad (20)$$

In [10], this entropy, which is a function of threshold  $t$ , is maximized and the corresponding gray level  $t$  is considered to be the optimum threshold value. Of course, this threshold is depending on  $q$  parameter. An example of thresholding is given in Figure 1 on the royalty-free image cameraman.jpg. In the same image we can see the histogram and the Tsallis entropy as a function of the chosen threshold. Since the final result depends on  $q$ , this coefficient can be used as an adjustable value and can play an important role as a tuning parameter [10]. As we can see in the example, the threshold is used to divide the data in two classes, the object and the background. In Figure 2, another example is given on lena.jpg.

Renyi entropy based image thresholding [13-15] and Tsallis entropy based image thresholding [10] are two important global threshold selection approaches in image segmentation. The equivalence relationship between these two approaches is revealed, that is, with the same parameter, the two approaches will obtain the same threshold.

In the previous discussion we have talk about gray tones. Of course images have colors: all what we have previously told can be applied to each of the colour tone (red, green and blue). In some previous papers [16-18], the reader can find an example of thresholding on color tones for a specific application: the digital restoration of manuscripts and drawings.

### 6. Multi-level thresholding

In computer vision and image processing, the reduction of a gray level image to a binary image can be obtained through a clustering-based image thresholding. Examples are given in the Figures 1 and 2. However, we can extend the method to multi-level thresholding.

Let us consider again an image having  $k$  gray levels, with a distribution of probabilities,  $p_1, p_2, \dots, p_k$ .

Let us assume some thresholds  $t_1, t_2, \dots, t_m$  for the

gray levels. Some classes must be introduced; their probability distributions are:

$$(1): \frac{p_1}{P_1}, \frac{p_2}{P_1}, \dots, \frac{p_{t_1}}{P_1} \quad (21)$$

$$(2): \frac{p_{t_1+1}}{P_2}, \frac{p_{t_1+2}}{P_2}, \dots, \frac{p_{t_2}}{P_2} \quad (22)$$

$$\dots$$

$$(m): \frac{p_{t_{m-1}+1}}{P_m}, \frac{p_{t_{m-1}+2}}{P_m}, \dots, \frac{p_{t_m}}{P_m} \quad (23)$$

$$(m+1): \frac{p_{t_m+1}}{P_{m+1}}, \frac{p_{t_m+2}}{P_{m+1}}, \dots, \frac{p_k}{P_{m+1}} \quad (24)$$

In (21)-(24), we have:

$$S_q = S_q^{(1)} + S_q^{(2)} + \dots + S_q^{(m+1)} + (1-q) \frac{1}{2} \sum_{i=1}^{m+1} \sum_{j=1; j \neq i}^{m+1} S_q^{(i)} S_q^{(j)} \\ + (1-q)^2 \frac{1}{6} \sum_{i=1}^{m+1} \sum_{j=1}^{m+1} \sum_{k=1}^{m+1} S_q^{(i)} S_q^{(j)} S_q^{(k)} + \dots + (1-q)^m S_q^{(1)} S_q^{(2)} \dots S_q^{(m+1)} \quad (29)$$

In [19], a multi-level thresholding in image segmentation is obtained combining Tsallis entropy and Particle Swarm Optimization (PSO). PSO is a computational method of optimization which use iterative tests to improve a candidate solution. In [20], the authors proposed the multi-level thresholding method for image segmentation, using the artificial bee colony approach to reduce the time of processing.

In the Figure 3, an example of multi-level thresholding using the Tsallis entropy is given. The upper left image shows cameraman.jpg in gray tones. On the right, we can see the effect of a thresholding, obtained by optimizing two thresholds using Tsallis entropy. The lower panel is showing the behavior of the entropy: in dark gray we can see the entropy as a function of threshold  $t_1$  for different values of the other threshold, in light gray, we can see the same for threshold  $t_2$ . Other two examples are proposed in the Figure 4.

## 7. The Two-Dimensional Histogram

As previously told,  $f(x,y)$  is the gray value of the pixel located at the point  $(x,y)$ . We can use, for segmentation, the average gray value of the

$$P_1 = \sum_{i=1}^{t_1} p_i; P_2 = \sum_{i=t_1+1}^{t_2} p_i; \dots; P_{m+1} = \sum_{i=t_m+1}^k p_i \quad (25)$$

The Tsallis entropy for each distribution and the total entropy are:

$$S_q^{(1)} = \frac{1}{q-1} \left\{ 1 - \sum_{i=1}^{t_1} \left( \frac{p_i}{P_1} \right)^q \right\} \quad (26)$$

$$S_q^{(2)} = \frac{1}{q-1} \left\{ 1 - \sum_{i=t_1+1}^{t_2} \left( \frac{p_i}{P_2} \right)^q \right\} \quad (27)$$

$$\dots$$

$$S_q^{(m+1)} = \frac{1}{q-1} \left\{ 1 - \sum_{i=t_m+1}^k \left( \frac{p_i}{P_{m+1}} \right)^q \right\} \quad (28)$$

neighborhood of each pixel too. Let  $g(x,y)$  be the average of the neighborhood of the pixel located at the point  $(x,y)$ . For instance, we can use the integer part of the arithmetic mean obtained with gray values of the given pixel at  $(x,y)$  and of its eight nearest neighboring pixels. While computing the average gray value, it is necessary to disregard the two rows from the top and bottom and two columns from the sides [15]. The gray value of the pixel,  $f(x,y)$ , and the average of its neighborhood,  $g(x,y)$ , are used to construct a two-dimensional histogram. The normalized histogram is approximated by using the formula is [15]:

$$h(i, j) = \frac{N_{ij}}{N_{tot}} \quad (30)$$

$N_{ij}$  is the number of pixels with gray value  $i$  and average gray value  $j$ , and  $N_{tot}$  is the number of pixels in the image.

Let us discuss the threshold to distinguish object and background. The threshold is obtained through a vector  $(t, s)$  where  $t$ , for  $f(x, y)$ , represents the

threshold of the gray level of the pixel and  $s$ , for  $g(x, y)$ , represents the threshold of the average gray level of the pixels neighborhood. Using (30), we find a surface that will have two peaks and one valley. The object and background correspond to the peaks and can be separated by selecting the vector  $(t, s)$  that maximizes a suitable criterion function  $U(t, s)$ .

Using vector  $(t, s)$ , the domain of the histogram is divided into four quadrants: first  $[t+1, k] \times [0, s]$ , second  $[0, t] \times [0, s]$ , third  $[0, t] \times [s+1, k]$ , and fourth quadrant  $[t+1, k] \times [s+1, k]$ . In [15], it is explained that two of the quadrants, first and third, contain information about edges and noise alone, and therefore they are ignored in the calculation. The quadrants which contain the object and the background are the second and fourth; they are considered to be independent distributions, the probability values in each case must be normalized in order to have a total probability equal to 1. The normalization is accomplished by using a posteriori class probabilities:

$$P_2(t, s) = \sum_{i=0}^t \sum_{j=0}^s h(i, j) \quad (31)$$

$$P_4(t, s) = \sum_{i=t+1}^k \sum_{j=s+1}^k h(i, j) \quad (32)$$

In [12], the contribution of the quadrants which contains the edges and noise is assumed negligible, hence it is approximated:

$$P_4(t, s) = 1 - P_2(t, s) \quad (33)$$

The distributions and entropies are:

$$A: \frac{h(0,0)}{P_2(t,s)}, \dots, \frac{h(0,s)}{P_2(t,s)}, \frac{h(1,0)}{P_2(t,s)}, \dots, \frac{h(t,s)}{P_2(t,s)} \quad (34)$$

$$B: \frac{h(t+1,s+1)}{P_4(t,s)}, \dots, \frac{h(t+1,k)}{P_4(t,s)}, \frac{h(t+2,s+1)}{P_4(t,s)}, \dots, \frac{h(k,k)}{P_4(t,s)} \quad (35)$$

$$S_q^A(t, s) = \frac{1}{q-1} \left\{ 1 - \sum_{i=1}^t \sum_{j=1}^s \left( \frac{h(i, j)}{P_2(t, s)} \right)^q \right\} \quad (36)$$

$$S_q^B(t, s) = \frac{1}{q-1} \left\{ 1 - \sum_{i=t+1}^k \sum_{j=s+1}^k \left( \frac{h(i, j)}{P_4(t, s)} \right)^q \right\} \quad (37)$$

Again, the total entropy is:

$$S_q(t, s) = S_q^A(t, s) + S_q^B(t, s) + (1-q) S_q^A(t, s) S_q^B(t, s) \quad (38)$$

The entropy (38) is a function of thresholds  $t$  and  $s$ ; we can find them maximizing the entropy. Parameter  $q$  can be used as a tuning parameter.

## 8. Discussion

As we have seen, Tsallis entropy is easy to use for discrete data and related frequencies. For this reason, it assumed a relevant role in several numerical applications. In particular we find it used in medical image processing, a quite dynamic branch of image processing [21]. This processing is based, among several other methods, on clustering the presence of unwanted lesions/regions in a noisy background and in highlighting the edges of poorly illuminated images. As a starting point of analysis, segmentation is often used. In [22], to set parameters on a segmentation based on pulse-coupled neural network (PCNN), the Tsallis entropy is used. Pulse-coupled networks are models proposed for high-performance biomimetic image processing.

Feature extraction method for image processing via PCNN and Tsallis entropy is presented in Ref.23 too. Some most recent papers using the Tsallis entropy in medical image processing are going from thresholding to the problem of image registration [24-27].

For what concerns the role of Tsallis entropy in the pattern recognition, Ref.28 compared the effectiveness of it over the classic Boltzmann–Gibbs–Shannon entropy and proposed a multi- $q$  approach to improve pattern analysis. Experiments in [28] show that the Tsallis entropy using the multi- $q$  approach has great advantages over the Boltzmann–Gibbs–Shannon entropy for pattern classification. Moreover, the approach is improving the image recognition rates. As explained in [28], this happens because the Tsallis entropy for different values of parameter  $q$  is encoding much more information from the given probability distribution than the Boltzmann–Gibbs–Shannon entropy.

## References

[1] Tsallis, C. (1988). Possible Generalization of Boltzmann-Gibbs Statistics. *Journal of Statistical Physics*, 52, 479-487.



- [2] Tsallis, C. (2009). Nonadditive Entropy and Nonextensive Statistical Mechanics - an Overview after 20 Years. *Braz. J. Phys.*, 39, 337-356.
- [3] Djerou, L., Khelil, N., Dehimi, N.H., & Batouche, M. (2012). Automatic Multi-Level Thresholding Segmentation Based on Multi-Objective Optimization. *Journal of Applied Computer Science & Mathematics*, 13 (6), 24-31.
- [4] Renyi, A. (1970). *Probability Theory*. North-Holland, Amsterdam.
- [5] Maszczyk, T., & Duch, W. (2008). Comparison of Shannon, Renyi and Tsallis Entropy Used in Decision Trees. *Artificial Intelligence and Soft Computing - ICAISC 2008*, 643-651, Springer Berlin Heidelberg.
- [6] Havrda, J., & Charvát, F., (1967). Quantification Methods of Classification Processes: Concept of Structural Alpha-Entropy. *Kybernetika (Prague)* 3, 95-100.
- [7] Sahoo, P.K., & Arora, G. (2006). Image Thresholding Using Two-Dimensional Tsallis- Havrda- Charvát. *Pattern Recognition Letters*, 27, 520-528.
- [8] Gull, S.F., & Skilling, J. (1984). Maximum Entropy Method in Image Processing. *Communications, Radar and Signal Processing*, IEE Proceedings F, 131(6), 646-659.
- [9] Yamano, T. (2001). Information Theory Based in Nonadditive Information Content. *Entropy* 3, 280-292; Yamano, T. (2000). *arXiv:cond-mat/0010074 [cond-mat.stat-mech]*
- [10] Portes de Albuquerque, M., Esquef, I.A., Gesualdi Mello, A.R., & Portes de Albuquerque, M. (2004). Image Thresholding Using Tsallis Entropy. *Pattern Recognition Letters*, 25(9), 1059-1065.
- [11] Sezgin, M., & Sankur, B. (2004). Survey over Image Thresholding Techniques and Quantitative Performance Evaluation. *Journal of Electronic Imaging*, 13(1), 146-165.
- [12] Kapur, J.N., Sahoo, P.K., & Wong, A.K.C. (1985). A New Method for Gray-Level Picture Thresholding Using the Entropy of the Histogram. *Comput. Vision Graphics Image Process.*, 29, 273-285.
- [13] Shitong Wang, & Chung, F.L. (2005). Note on the Equivalence Relationship between Renyi-Entropy Based and Tsallis-Entropy Based Image Thresholding. *Pattern Recognition Letters*, 26(14), 2309-2312.
- [14] Sahoo, P., Wilkins, C., & Yeager, J. (1997). Thresholding Selection Using Renyi's Entropy. *Pattern Recognition*, 30 (1), 71-84.
- [15] Sahoo, P.K., & Arora, G. (2004). A Thresholding Method Based on Two Dimensional Renyi's Entropy. *Pattern Recognition*, 37 (6), 1149-1161.
- [16] Sparavigna, A. (2009). The Digital Restoration of Da Vinci's Sketches. *arXiv:0903.1448 [cs.CV]*
- [17] Sparavigna, A.C. (2011). An Image Processing of a Raphael's Portrait of Leonardo. *arXiv:1111.6030 [cs.CV]*
- [18] Sparavigna, A.C. (2011). Portraits of Leonardo da Vinci. *Archaeogate*, 6 December 1011.
- [19] Sathya, P. D., & Kayalvizhi, R. (2010). PSO-based Tsallis Thresholding Selection Procedure for Image Segmentation. *International Journal of Computer Applications*, 5(4), 39-46.
- [20] Yudong Zhang, & Lenan Wu, Optimal Multi-Level Thresholding Based on Maximum Tsallis Entropy via an Artificial Bee Colony Approach. *Entropy* 2011, 13(4), 841-859
- [21] Tamalika Chaira (2015). *Medical Image Processing: Advanced Fuzzy Set Theoretic Techniques*. CRC Press.
- [22] Shi Weili, Miao Yu, Chen Zhanfang, & Zhang Hongbiao (2009). Research of Automatic Medical Image Segmentation Algorithm Based on Tsallis Entropy and Improved PCNN. *International Conference on Mechatronics and Automation, ICMA 9-12 August 2009*, 1004-1008.
- [23] Yudong Zhang, & Lenan Wu (2008). Pattern Recognition via PCNN and Tsallis Entropy. *Sensors*, 8(11), 7518-7529.
- [24] El-Sayed, M.A., Abdel-Khalek, S. & Abdel-Aziz, E. (2011). Study of Efficient Technique Based on 2D Tsallis Entropy for Image Thresholding. *International Journal on Computer Science and Engineering (IJCSE)*, 3(9), 3125-3138.
- [25] Ramirez-Villegas, J.F., & Ramirez-Moreno, D.F. (2012). Wavelet Packet Energy, Tsallis Entropy and Statistical Parameterization for Support Vector-Based and Neural-Based Classification of Mammographic Regions. *Neurocomputing*, 77(1), 82-100.
- [26] El-Sayed, M.A. (2011). A New Algorithm Based Entropic Threshold for Edge Detection in Images. *IJCSI - International Journal of Computer Science Issues*, 8(5), 71-78.
- [27] Khader, M. & Ben Hamza, A. (2012). An Information-Theoretic Method for Multimodality Medical Image Registration. *Expert Systems with Applications*, 39(5), 5548-5556.
- [28] Fabbri, R., Gonçalves, W.N., Lopes, F.J.P., & Bruno, O.M. (2012). Multi-q Pattern Analysis: A Case Study in Image Classification. *Physica A: Statistical Mechanics and its Applications*, 391(19), 4487-4496.

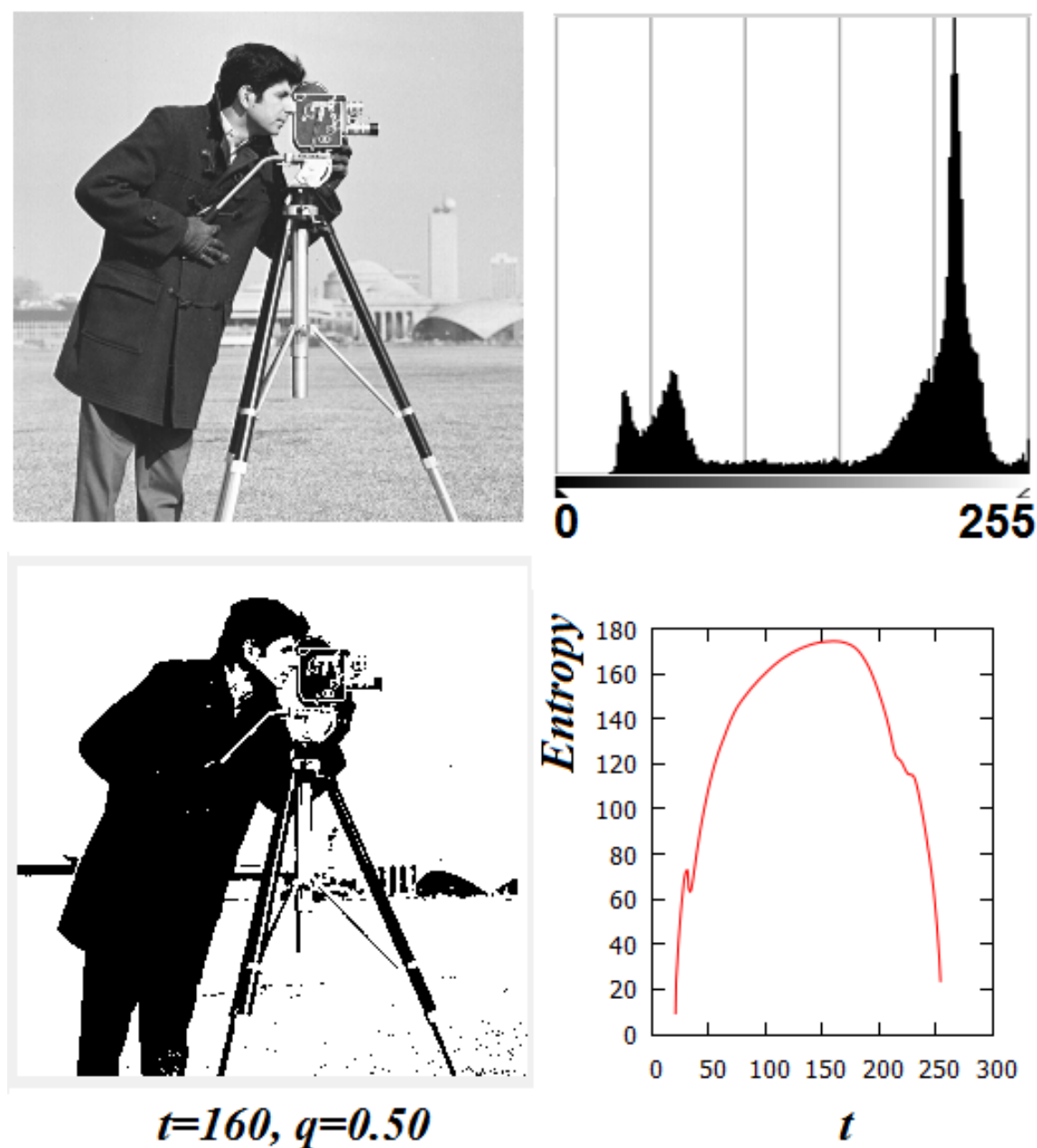


**Figure 1:** An example of bi-level thresholding using Tsallis entropy. The upper left image shows cameraman.jpg in gray tones. On the right, we can see the histogram of this image, obtained using GIMP (GNU Image Manipulation Program). In the lower part, we can see the effect of a thresholding, obtained by maximizing the Tsallis entropy. The pixels having a gray tone larger than the threshold value become white; the pixels having a lower value become black. On the right, we can see the behavior of Tsallis entropy as a function of threshold. The maximum value corresponds to 160. Let us note that changing parameter  $q$ , the threshold is different, such as the values of entropy.



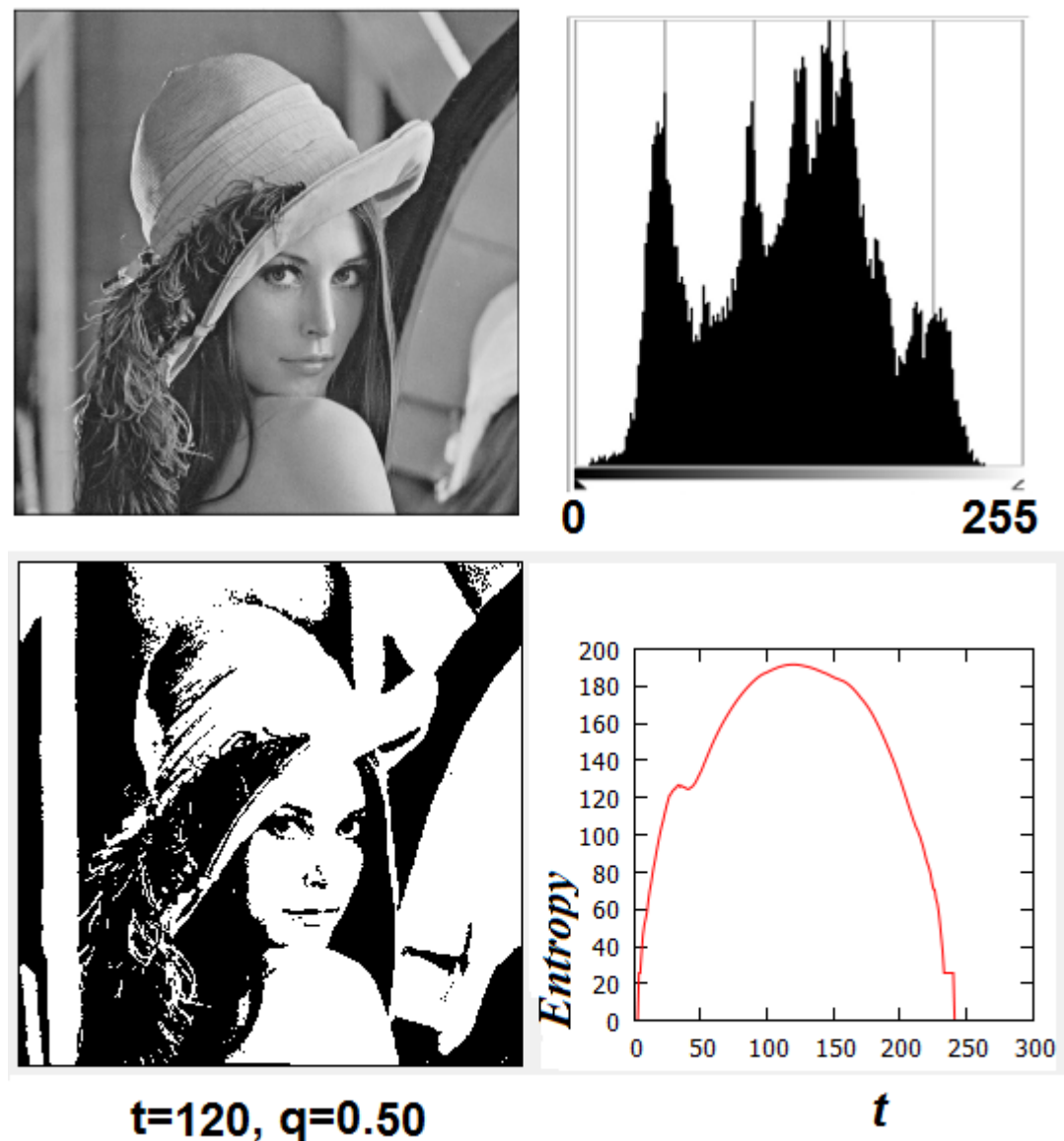


**Figure 2:** Another example of bi-level thresholding using the Tsallis entropy. The upper left image shows lena.jpg in gray tones. On the right, we can see the histogram of this image. In the lower part, we can see the effect of thresholding, obtained using Tsallis entropy. On the right, we can see the behavior of Tsallis entropy as a function of threshold. The maximum value corresponds to 120.



$$t_1=94, t_2=175, q=0.5$$

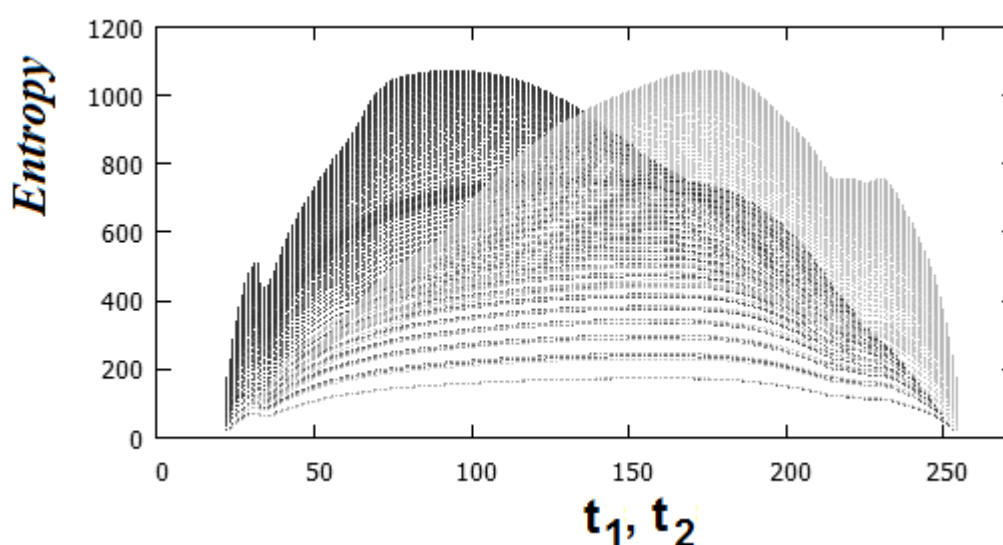


**Figure 3:** An example of multi-level thresholding using Tsallis entropy (three levels). The upper left image shows cameraman.jpg in gray tones. On the right, we can see the effect of thresholding. The lower panel is showing the behavior of the entropy: in dark gray we can see the entropy as a function of threshold  $t_1$ , for different values of the other threshold; in light gray, we can see the same for threshold  $t_2$ .

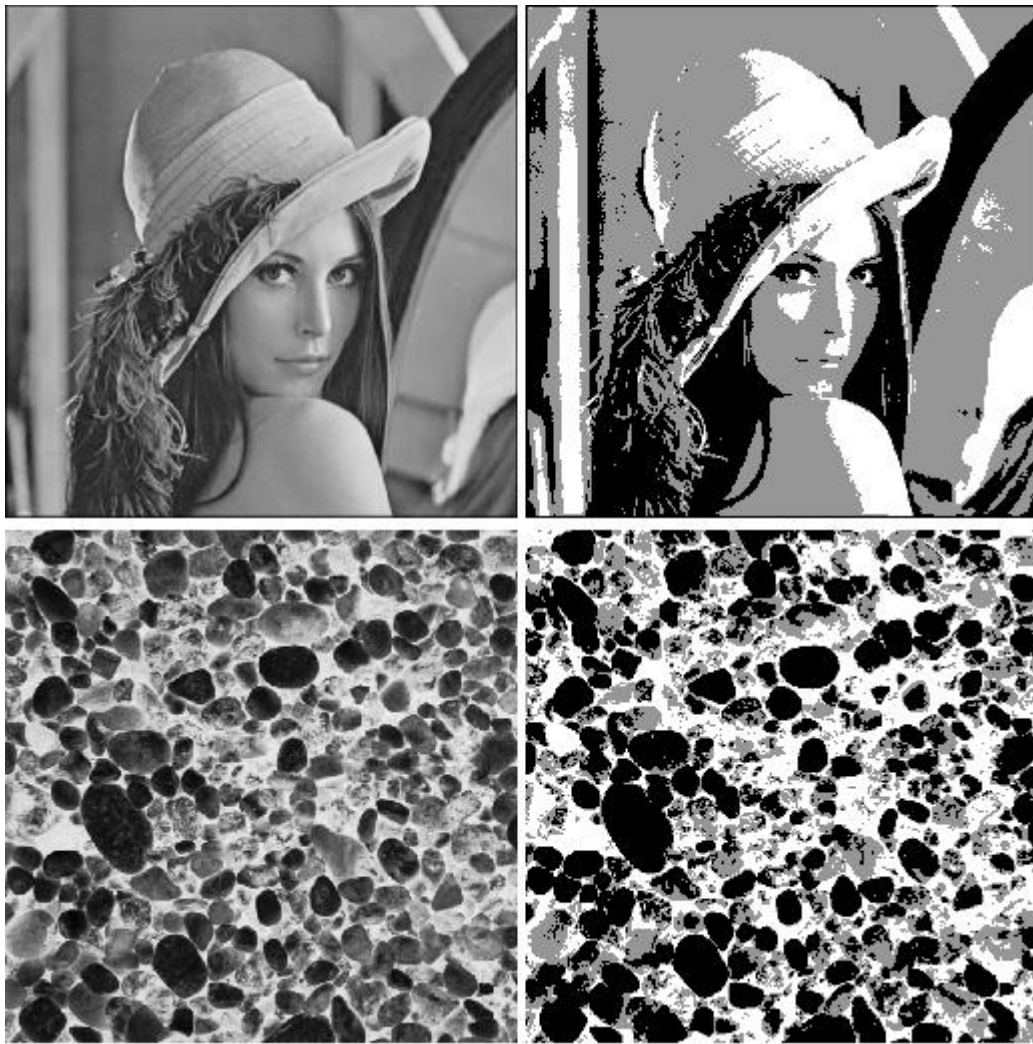


**Figure 4:** Two examples of multi-level thresholding using the Tsallis entropy (three levels). The upper image on the left is lena.jpg, the lower image D23.jpg from Brodatz album.